CRYSTAL GROWTH & DESIGN

Article

pubs.acs.org/crystal

# Conformational Heterogeneity, Self-Assembly, and Gas Adsorption Studies of Isomeric Hybrid Peptides

Sibaprasad Maity, Poulami Jana, Suman Kumar Maity, Pankaj Kumar, and Debasish Haldar*

Department of Chemical Sciences, Indian Institute of Science Education and Research - Kolkata, Mohanpur, West Bengal 741252, India

Supporting Information

**ABSTRACT:** The folding and self-assembly propensities of three synthetic isomeric aliphatic–aromatic backbone hybrid peptides are illustrated. Single crystal X-ray diffraction studies of three isomeric hybrid dipeptides Boc-Phe-x-aminobenzoic acid (x = o/m/p) reveal that the peptides adopt unconventional conformations which self-assemble to form diverse supramolecular architectures using hydrogen bonding interactions and other noncovalent interactions in the solid state. The $N_2$ sorption propensities of the isomeric hybrid peptides in the solid state significantly vary with folding and self-assembly nature. The peptides **1** and **2** exhibit type-III $N_2$ sorption isotherm, though peptide **1** adsorbs 2-fold higher $N_2$ than does peptide **2**.

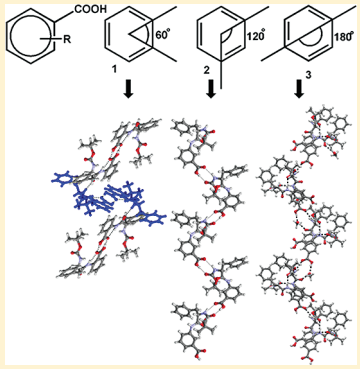


## INTRODUCTION

Developing biomimetic materials, such as the folded structures of biopolymers, by the self-assembly of synthetic organic moieties is highly interesting due to their potential application in bioorganic chemistry and material sciences.[1] The self-assembly process requires a combination of several noncovalent interactions such as hydrogen bonding, $\pi-\pi$ stacking, and van der Waals interactions between the building blocks.[2] In this context, the small peptide scaffold that can occasionally serve as a hydrogen bond donor or acceptor is highly interesting.[3] This interest stems from their structural versatility, biocompatibility, robustness, and accessibility by standard analytical methods.[4] The folding patterns of the scaffolds mostly belong to the canonical folds.[5] Görbitz has reported the supramolecular left-handed double helices (Val-Ala class structures) from hydrophobic dipeptides from $\alpha$-amino acids.[3,6] Majority of the reports of unconventional folds have exploited scaffold combinations of aliphatic and aromatic backbone moieties.[7] Huc and co-workers have reported the formation of a herringbone helix from noncanonical folding of an aromatic–aliphatic $\delta$-peptides.[8] Lin et al. has discussed the construction of a two-dimensional (2D) herringbone-like zinc coordination polymer from a helical motif.[9] Tomasini et al. has reported formation of fiberlike structures from synthetic Boc-Phe containing di- or tripeptides.[10]

Over the past few years, our research group has dealt with the supramolecular materials from short synthetic peptides.[11] Herein we present the noncanonical folding and formation of diverse supramolecular structures in the solid state from isomeric aromatic–aliphatic backbone hybrid dipeptides (**1**–**3**), each containing N-terminal L-phenylalanine and C-terminal rigid aromatic $\beta/\gamma/\delta$ amino acids. The molecular scaffold Boc-Phe-x-aminobenzoic acid (x = $o/m/p$) adopt unconventional conformations in the solid state and form a supramolecular herringbone helix or single helix or corrugated sheetlike structure in higher order assembly, directed by intermolecular N–H···O and O–H···O hydrogen bonds. Moreover, the peptides exhibit type-III $N_2$ sorption isotherm. The sorption propensities of the isomeric peptides differ significantly with folding and self-assembly pattern.

## RESULTS AND DISCUSSION

**Background.** Three N-terminally protected dipeptides, Boc-Phe-x-aminobenzoic acid (x = $o/m/p$) containing N-terminal L-phenylalanine and C-terminal rigid aromatic $\beta/\gamma/\delta$ amino acids residues have been synthesized by conventional solution-phase methodology, purified, characterized, and studied (Figure 1). The peptides have been designed with aromatic $\beta$, $\gamma$, $\delta$ amino acids to increase the helical pitch and decrease the number of residues per supramolecular helical turn (Figure 1). Colorless monoclinic crystals of peptides **1**, **3**, and colorless orthorhombic crystals of peptide **2** suitable for X-ray diffraction studies were obtained from their methanol–water solutions by slow evaporation.

The conformational heterogeneity of the aliphatic–aromatic backbone hybrid isomeric peptides was observed by the solid state FTIR spectroscopy. The region 1800–1500 $cm^{-1}$ is important for the stretching band of amide I, the bending peak of amide II, and the hydrogen bonded urethane groups.[12] Another informative frequency range is 3500–3200 $cm^{-1}$,

Received: September 26, 2011
Revised: November 15, 2011
Published: November 29, 2011

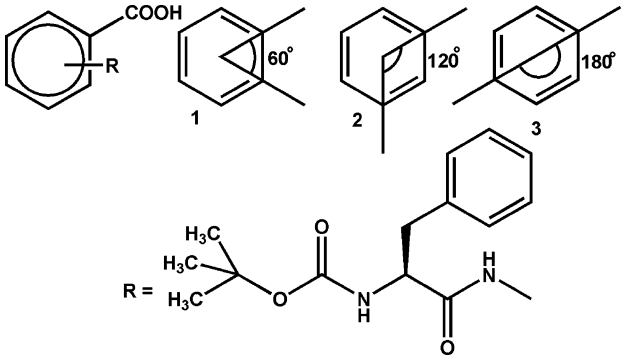


**Figure 1.** The schematic presentation of the reported dipeptides **1**−**3**.

corresponding to the N−H stretching vibrations of the peptide.[13] The FTIR studies show that the peptides molecules are strongly intermolecular hydrogen bonded in the solid state (Figure 2). Intense bands at 3316 (peptide **1**) $cm^{-1}$, 3312

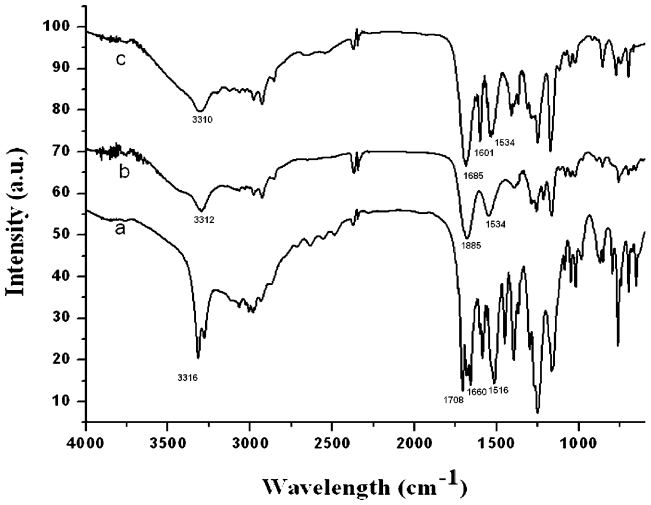


**Figure 2.** The solid state FTIR spectrum of the reported dipeptides (a) **1**, (b) **2**, and (c) **3**.

(peptide **2**) $cm^{-1}$, and 3310 (peptide **3**) $cm^{-1}$ were observed for the reported peptides, indicating the presence of strongly hydrogen-bonded NH groups.[13] The characteristic IR absorption bands at about 1516 $cm^{-1}$, 1650 $cm^{-1}$, 1708 $cm^{-1}$ for peptide **1** and 1534 $cm^{-1}$, 1685 $cm^{-1}$ for peptide **2** and **3** suggest the conformational heterogeneity between the isomeric peptides.

**Crystal Structure Analysis.** Peptide **1** crystallizes with four peptide molecules in the asymmetric unit (Figure ESI 1), whereas peptide **2** crystallizes with one peptide molecule. However, two molecules of peptide **3** crystallize with two molecules of methanol in the asymmetric unit (Figure ESI 1). Interestingly, the torsion angle around the phenylalanine residue appears to play a critical role in dictating the overall structural features. From the crystal structure of peptide **1**, it is evident that there are two intramolecular hydrogen bonds. For each of peptide **1** molecule in the asymmetric unit, the five-member hydrogen bonded ring between Phe N and anthranelic acid NH and the six-member hydrogen bonded ring between anthranelic acid NH and anthranelic acid C═O resulting a rigid conformation in the solid state (Figure 3a).[14] The backbone torsion angles ($\phi$, $\psi$) of peptide **1** molecules are

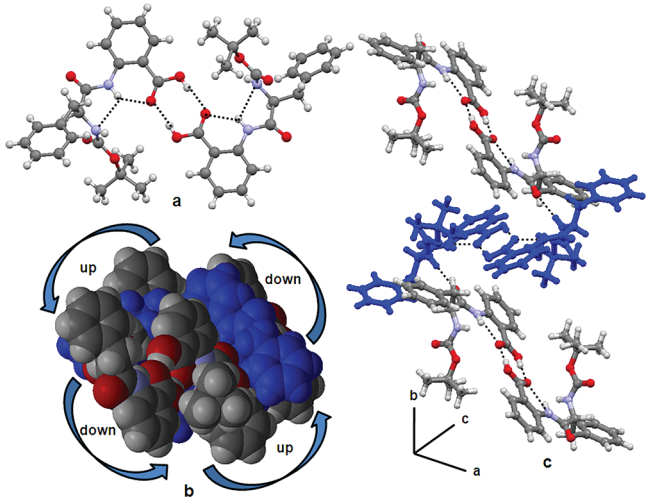


**Figure 3.** (a) The hydrogen bonded dimer of peptide **1A·D**; (b) top view; and (c) side view of supramolecular noncanonical herringbone helix.

listed in Table 1. Further, the peptide **1A** molecule forms an intermolecular hydrogen bond with peptide **1D** molecule (O4−

**Table 1. The Important Backbone Torsion Angles (°) of Peptide 1−3**

| peptide | $\phi$1 | Ψ1 | $\phi$2 | Ψ2 |
|---|---|---|---|---|
| Peptide **1A** | 62.05 | 37.97 | −179.72 | −179.18 |
| Peptide **1B** | 63.63 | 36.38 | 169.52 | 179.35 |
| Peptide **1C** | −77.82 | −31.52 | −161.96 | −177.97 |
| Peptide **1D** | −78.17 | −31.05 | 177.13 | 179.03 |
| Peptide **2** | −59.00 | 135.31 | 37.18 | −161.15 |
| Peptide **3A** | −72.68 | 158.79 | 19.04 | 5.33 |
| Peptide **3B** | −111.66 | 152.52 | −7.07 | −177.89 |

H4···O9, 1.85 Å, 2.71 Å, 166°, 1 + *x*, *y*, 1 + *z*) and (O10−H10A···O5, 1.90 Å, 2.71 Å, 166°, −1 + *x*, *y*, −1 + *z*) to form a dimer like a traditional acid dimer (Figure 3a). Similarly, the peptide **1B** molecule forms an acid dimer with the peptide **1C** molecule. In higher order assembly, the dimeric building blocks of peptide **1** self-assemble through intermolecular hydrogen bonding interactions (N1−H1···O8, 2.14 Å, 2.84 Å, 155°, 1 − *x*, −1/2 + *y*, 1 − *z* and (N3−H3···O8, 2.00 Å, 2.73 Å, 142°, −*x*, 1/2 + *y*, 1 − *z*)) to form a supramolecular herringbone like helical architecture along the axis parallel to the crystallographic *b* direction (Figure 3b,c).[15] In higher order packing, the peptide **1** forms a herringbone like architecture by hydrogen bonding interaction (Figure ESI 2).

In comparison with peptide **1**, peptide **2** contains the terminal acid functional group at the meta position, but this change had a significant impact on the molecular conformation. As it is evident from the solid state structure, the BOC amide functional group adopts cis geometry (Figure 4) which is very rare. In peptide **2**, there is no intramolecular hydrogen bond and no acid dimer formation like peptide **1**. The backbone torsion angles (Table 1) of peptide **2** are significantly different to that of peptides **1** and **3**. Moreover, in higher order packing, the individual peptide **2** molecules are themselves regularly interlinked through intermolecular hydrogen bonding interactions (N1−H1···O4, 2.1 Å, 2.93 Å, 161°, −1 − *x*, 1/2 + *y*, 1/2 − *z* and O5−H5···O2, 1.84 Å, 2.65 Å, 167°, −1 − *x*, −1/2 +


dx.doi.org/10.1021/cg201268x | *Cryst. Growth Des.* 2012, 12, 422−428

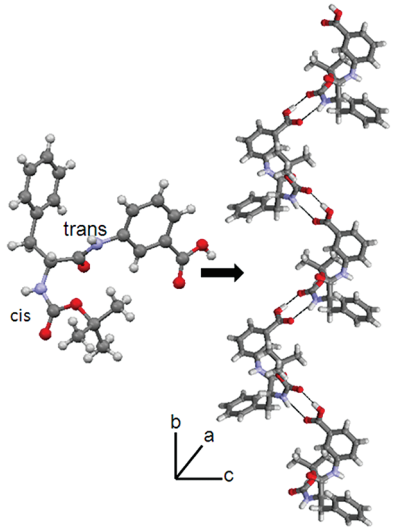


**Figure 4.** The *cis* amide configuration and supramolecular helical structures obtained from peptide **2**.

*y*, 1/2 − *z*) and thereby form a supramolecular single helix along the *b* axis (Figure 4).[16]

From crystal data, the asymmetric unit contains two molecules of peptide **3** and two molecules of methanol. The backbone torsion angles of molecules A and B of peptide **3** are significantly different (Table 1). For peptide **3**, in the asymmetric unit, the dimer formed by intermolecular hydrogen bonds N2−H2···O7, 2.00 Å, 2.83 Å, 164° and N4−H4···O2, 2.14 Å, 2.98 Å, 168° (Figure 5).

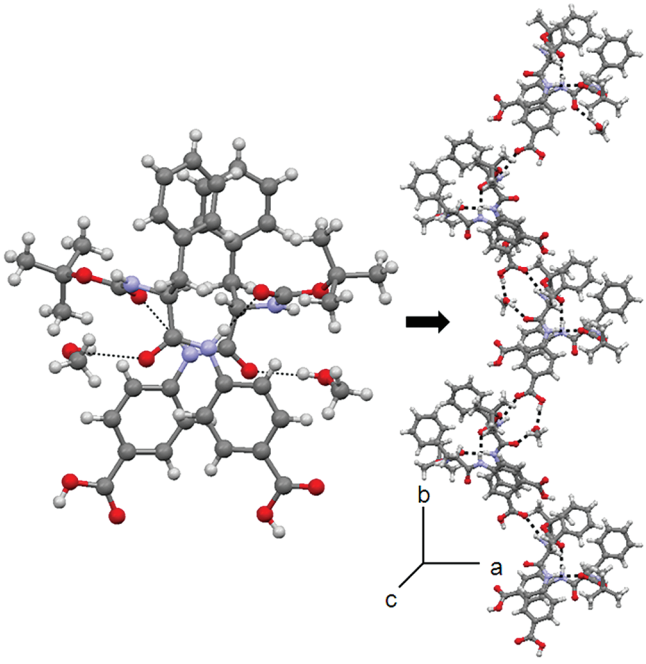


**Figure 5.** Formation of methanol mediated supramolecular corrugated sheetlike structure from peptide **3**.

The peptide molecules are bound with methanol by intermolecular hydrogen bonding interactions (O11−H11A···O8, 1.93 Å, 2.75 Å, 171° and O12−H12A···O3, 2.09 Å, 2.86 Å, 156°) (Figure 5). There are also two $\pi-\pi$ interactions between Paba rings (shortest C−C distance 3.75 Å) and phenylalanine rings (shortest C−C distance 4.11 Å) in the dimer. Each of peptide **3** dimers stacked by maintaining the proper registry to form a corrugated sheetlike structure through intermolecular hydrogen bonding interactions (N1−H1···O4, 2.05 Å, 2.90 Å, 169°, *x*, *y*, 1 + *z* and N3−H3···O9, 2.26 Å, 3.02 Å, 148°, 2 − *x*, −1/2 + *y*, 1 − *z*) along with the intervening bridging methanol molecules (O5−H5···O12, 1.84 Å, 2.65 Å, 173°, *x*, *y*, −1 + *z* and O10−H10A···O11, 1.77 Å, 2.58 Å, 169°, 2 − *x*, 1/2 + *y*, 1 − *z*) (Figure 5). Hydrogen bonding data for peptides **1**−**3** are also listed in Table 2. Crystal data for these three hybrid peptides are detailed in Table 3.

**Table 2. Hydrogen Bonds in Crystal Structures of Peptide 1−3**

| interactions | H···A/Å | D···A/Å | D−H···A/deg | |
|---|---|---|---|---|
| Peptide **1** | | | | |
| N1−H1···O8 | 2.14 | 2.94 | 155 | 1 − x, −1/2+ y, 1 − z |
| N2−H2···O5 | 1.97 | 2.66 | 136 | intramolecular |
| N2−H2···N1 | 2.37 | 2.78 | 110 | intramolecular |
| N3−H3···O3 | 2.00 | 2.72 | 142 | −x, 1/2 + y, 1 − z |
| O4−H4···O9 | 1.86 | 2.65 | 166 | 1 + x, y, 1 + z |
| N4−H4D···O9 | 1.96 | 2.65 | 137 | intramolecular |
| N4−H4D···N3 | 2.35 | 2.78 | 111 | intramolecular |
| N5−H5···O20 | 2.20 | 2.90 | 138 | −x, 1/2 + y, 1 − z |
| N6−H6A···O14 | 2.11 | 2.74 | 131 | intramolecular |
| N6−H6A···N5 | 2.40 | 2.80 | 109 | intramolecular |
| N7−H7···O13 | 1.95 | 2.75 | 155 | 2 − x, −1/2 + y, 1 − z |
| N8−H8···O17 | 1.95 | 2.65 | 138 | intramolecular |
| N8−H8···N7 | 2.31 | 2.72 | 110 | intramolecular |
| O10−H10A···O5 | 1.90 | 2.70 | 166 | x, y, −1 + z |
| O18−H18A···O14 | 1.88 | 2.70 | 176 | x, −1 + y, z |
| Peptide **2** | | | | |
| N1−H1···O4 | 2.11 | 2.93 | 161 | −1 + x, y, z |
| N2−H2···O3 | 2.51 | 3.31 | 157 | 1 + x, y, z |
| O5−H5···O2 | 1.84 | 2.64 | 167 | −1 − x, −1/2 + y, 1/2 − z |
| Peptide **3** | | | | |
| N1−H1···O4 | 2.05 | 2.90 | 169 | x, y, 1 + z |
| N2−H2···O7 | 2.00 | 2.83 | 164 | intramolecular |
| N3−H3···O9 | 2.26 | 3.02 | 148 | 2 − x, −1/2 + y, 1 − z |
| N4−H4···O2 | 2.14 | 2.98 | 168 | intramolecular |
| O5−H5···O12 | 1.84 | 2.65 | 173 | x, y, −1 + z |
| O10−H10A···O11 | 1.77 | 2.58 | 169 | 2 − x, 1/2 + y, 1 − z |
| O11−H11A···O8 | 1.93 | 2.74 | 171 | intramolecular |
| O12−H12A···O3 | 2.09 | 2.86 | 156 | intramolecular |

**Thermal Characterization.** The TGA-DTG experiments also support the different nature of the reported isomeric dipeptides (Figure 6). The TGA results show no decomposition or mass loss up to 157 and 178 °C for peptides **1** and **2**, respectively. For peptide **3**, there is a mass loss at 87 °C for release of methanol and decomposition at 166 °C.

**$N_2$ Gas Adsorption.** In order to examine the void and hollow in the noncanonical folded structure and self-assembly, gas adsorption studies have been performed.[17] The $N_2$ sorption studies with evacuated sample of peptides **1** and **2** exhibit type-III isotherm (Figure 7). The $N_2$ uptake of peptide **1** crystal was found to be 22 $cm^3/g$; however that for peptide **2** is 11 $cm^3/g$


dx.doi.org/10.1021/cg201268x | *Cryst. Growth Des.* 2012, 12, 422−428

Table 3. Crystallographic Parameters of Peptides 1−3

| | Peptide 1 | Peptide 2 | Peptide 3 |
|---|---|---|---|
| empirical formula | C21H24N2O5 | C21H24N2O5 | C21H24N2O5,CH4O |
| formula weight | 384.42 | 384.42 | 416.47 |
| crystal system | monoclinic | orthorhombic | monoclinic |
| space group | $P2_1$ | $P2_12_12_1$ | $P2_1$ |
| $T$ (K) | 100 | 100 | 100 |
| $a$/Å | 10.578(4) | 5.507(4) | 9.412(8) |
| $b$/Å | 11.874(5) | 17.177(12) | 22.041(19) |
| $c$/Å | 32.517(13) | 21.103(16) | 11.901(10) |
| $\alpha$/deg | 90 | | 90 |
| $\beta$/deg | 94.155 | | 109.25 |
| $\gamma$/deg | 90 | | 90 |
| $V$/Å$^3$ | 4073.5 | 1996.3 | 2330.8 |
| $Z$ | 8 | 4 | 4 |
| $D_c$ Mg m$^{-3}$ | 1.253 | 1.279 | 1.187 |
| reflns collected | 22876 | 22927 | 18704 |
| unique reflns | 13428 | 4239 | 9813 |
| observed reflns | 7272 | 3074 | 6410 |
| $R_1$ $I > 2\sigma(I)$ | 0.0880 | 0.0438 | 0.0473 |
| $wR_2$ | 0.2402 | 0.0874 | 0.1509 |

indicating that the supramolecular herringbone like helical packing of peptide **1** provides a larger void (3.02 nm) than the supramolecular single helical packing of peptide **2** (2.84 nm). On evacuation peptide **3** crystals released methanol molecules and formed an opaque polymorph. Hence, for peptide **3**, the $N_2$ sorption study was not performed.

**Morphology.** To obtain insight about the morphology of the reported isomeric peptides, field-emission scanning electron microscopic (FE-SEM) measurements were carried out. For FE-SEM experiments, dilute solutions (0.5 mM) of reported peptides in methanol−water (1:1 v/v) were placed on a microscopic glass slide and then dried under a vacuum for two days. Figure 8 depicts the FE-SEM images of the aliphatic−aromatic backbone hybrid isomeric peptides. From Figure 8a,b, the micrographs show the roselike morphology for peptide **1** in the self-assembled state. Peptides **2** and **3** exhibit twisted fiberlike morphology (Figure 8, panels c and d respectively) with a diameter ca. 100 nm and several micrometers in length.

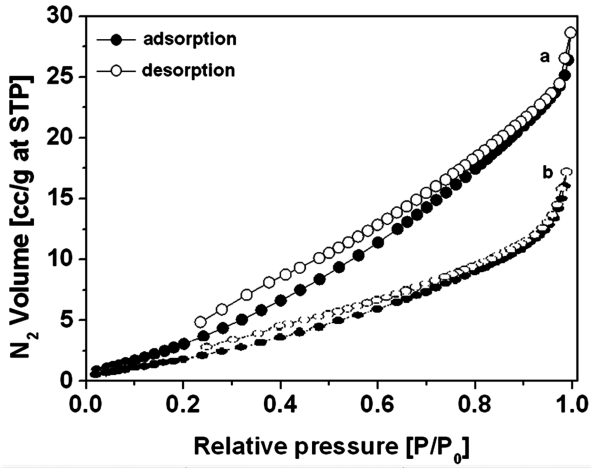


Figure 7. $N_2$ sorption isotherm of (a) peptide **1** and (b) peptide **2** at STP ($P_0$ = 1 atm) showing the sorption is 2-fold higher for peptide **1**.

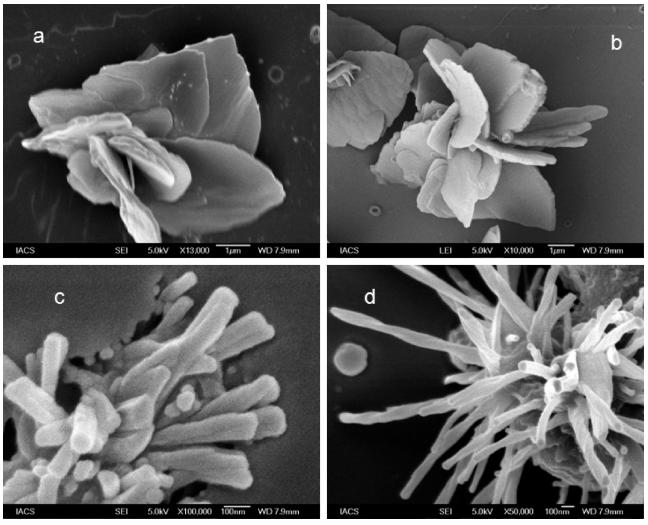


Figure 8. FE-SEM images (a) and (b) exhibit roselike morphology of peptide **1** and (c) and (d) showing twisted fiberlike morphology of peptides **2** and **3**, respectively.

## CONCLUSION

In conclusion, we have shown that the isomeric aliphatic−aromatic backbone hybrid peptides adopt unconventional

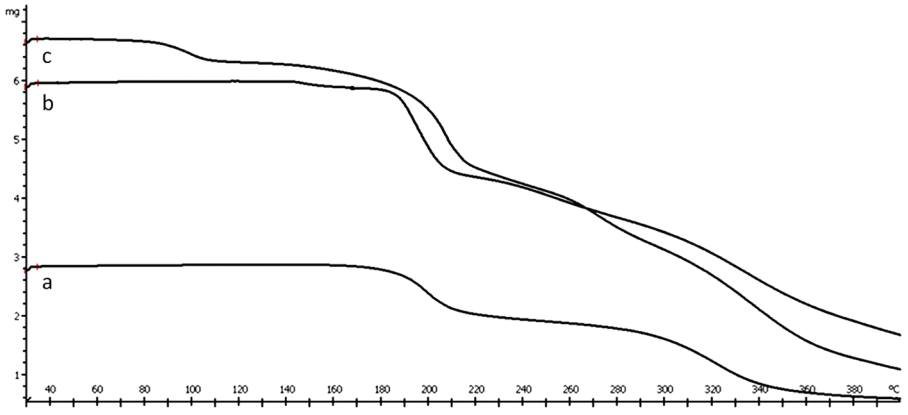


Figure 6. TGA of (a) peptide **1**, (b) peptide **2**, and (c) peptide **3**. From this graph, the peptide **1** and **2** exhibit no decomposition, phase transitions, or mass loss up to 157 and 178 °C, respectively. The crystal of peptide **3** has released methanol at 87 °C and decomposed at 166 °C.


dx.doi.org/10.1021/cg201268x | Cryst. Growth Des. 2012, 12, 422−428

conformations and exhibit diverse self-assembly directed by intermolecular hydrogen bonds. In crystals, the ortho isomer self-assemble to form a supramolecular herringbone-like helix, whether the meta isomer exhibits a helical tapelike structure and para isomer shows corrugated sheetlike architecture. Moreover, peptide **1** crystals adsorb $N_2$ 2-fold higher than does peptide **2**. Such noncanonical folding and assembly may foster new studies for the design of useful materials.

## EXPERIMENTAL SECTION

**General.** All amino acids (L-phenylalanine, *o*-aminobenzoic acid, *m*-aminobenzoic acid, *p*-aminobenzoic acid) were purchased from Sigma chemicals. 1-Hydroxybenzotriazole (HOBt) and dicyclohexylcarbodiimide (DCC) were purchased from SRL.

**Synthesis.** The peptides were synthesized by conventional solution-phase methodology by using a racemization free fragment condensation strategy. The Boc group was used for N-terminal protection, and the C-terminus was protected as a methyl ester. Couplings were mediated by DCC/HOBt. Deprotection of the methyl ester was performed using the saponification method. All the intermediates were characterized by 500 MHz and 400 MHz $^1$H NMR, $^{13}$C NMR, and mass spectrometry. The final compounds were fully characterized by 500 MHz and 400 MHz $^1$H NMR spectroscopy, $^{13}$C NMR spectroscopy (125 MHz, 100 MHz), mass spectrometry, and IR spectroscopy. Peptide **1**−**3** were also characterized by X-ray crystallography.

*(a). Boc-Phe-Anthra-OMe* ***4***. 3.714 g (14 mmol) of Boc-Phe-OH was dissolved in 30 mL of dry DCM in an ice−water bath. H-Anthra-OMe was isolated from 5.628 g (30 mmol) of the corresponding methyl ester hydrochloride by neutralization, and subsequent extraction with ethyl acetate and ethyl acetate extract was concentrated to 15 mL. It was then added to the reaction mixture, followed immediately by 2.888 g (14 mmol) of dicyclohexylcarbodiimide (DCC) and 1.891 g (14 mmol) of HOBt. The reaction mixture was allowed to come to room temperature and was stirred for 48 h. DCM was evaporated and the residue was dissolved in ethyl acetate (60 mL) and dicyclohexylurea (DCU) was filtered off. The organic layer was washed with 2 M HCl (3 × 50 mL), brine (2 × 50 mL), 1 M sodium carbonate (3 × 50 mL), and brine (2 × 50 mL) and dried over anhydrous sodium sulfate, and evaporated in a vacuum to yield compound **4** as a white solid. The product was purified by silica gel (100−200 mesh) using n-hexane−ethyl acetate (3:1) as the eluent.

Yield: 4.574 g (10.68 mmol, 76.35%).

$^1$H NMR ($CDCl_3$, 400 MHz, $\delta_{ppm}$): 11.410 (s, 1H, NH Anthra), 8.72−8.70 (d, 1H, $J$ = 8 Hz, anthra ring proton), 8.00−7.98 (d, 1H, $J$ = 8 Hz, anthra ring proton), 7.54−7.53 (m, 1H, anthra ring proton), 7.26−7.25 (m, 5H, phenyl ring proton), 7.22 (m, 1H, anthra ring proton), 5.05 (d, 1H, $J$ = 6 Hz, Phe NH), 4.57 (m, 1H, C$\alpha$H Phe), 3.86 (s, 3H, OMe), 3.21−3.20 (d, 2H, $J$ = 10 Hz, C$\beta$H Phe), 1.43 (s, 9H, Boc). $^{13}$C NMR ($CDCl_3$, 100 MHz, $\delta_{ppm}$): 170.534, 168.169, 155.183, 140.719, 136.305, 134.531, 130.784, 129.306, 128.658, 126.913, 122.82, 120.363, 115.405, 80.146, 56.863, 52.257, 38.461, 28.268. FTIR (cm$^{-1}$): 3305, 3272, 2927, 1724, 1700, 1672, 1585, 1527, 1508, 1448, 1298, 1272.

Anal. Calcd for $C_{22}H_{26}N2O_5$ (398.45): C, 66.32; H, 6.58; N, 7.03; Found: C, 66.40; H, 6.55; N, 7.05.

*(b). Boc-Phe-Anthra-OH* ***1***. To 4.183 g (10.5 mmol) of Boc-Phe-Antra-OMe, 25 mL of MeOH and 15 mL of 2 M NaOH were added, and the progress of saponification was monitored by thin layer chromatography (TLC). The reaction mixture was stirred. After 10 h, methanol was removed under a vacuum; the residue was dissolve in 50 mL of water, and washed with diethyl ether (2 × 50 mL). Then the pH of the aqueous layer was adjusted to 2 using 1 M HCl and it was extracted with ethyl acetate (3 × 50 mL). The extracts were pooled, dried over anhydrous sodium sulfate, and evaporated under a vacuum to obtain the compound as a white solid.

Yield 3.690 g (9.60 mmol, 91.45%).

Melting point: 162 °C

$^1$H NMR (DMSO-$d_6$, 500 MHz, $\delta_{ppm}$): 12.18 (s, 1H, COOH), 8.62−8.60 (m, 1H, anthra ring proton), 8.01−8.00 (d, 1H, anthra ring proton), 7.56−7.52 (m, 1H, anthra ring proton), 7.43−7.42 (d, 1H, anthra ring proton), 7.31 (s, 1H, anthra NH), 7.29−7.14 (m, 5H, phenyl ring protons), 7.19 (d, 1H, $J$ = 5, Phe NH), 4.20−4.18 (m, 1H, C$\alpha$H Phe), 3.22−3.18 (d, 1H, $J$ = 20 Hz, C$\beta$H Phe), 2.91−2.86 (d, 1H, $J$ = 20 Hz, C$\beta$H Phe), 1.31 (s, 9H, Boc). $^{13}$C NMR (DMSO-*d6*, 125 MHz, $\delta_{ppm}$): 170.95, 169.34, 155.46, 140.54, 138.28, 133.29, 131.13, 129.03, 128.09, 126.20, 122.44, 119.26, 117.85, 78.33, 57.75, 36.69, 28.05, 27.71. FTIR (cm$^{-1}$): 3316, 3279, 1708, 1683, 1659, 1587, 1516, 1451, 1396, 1299, 1252, 1167.

Anal. calcd for $C_{21}H_{24}N_2O_5$ (384.43): C, 65.61; H, 6.29; N, 7.29.

Found: C, 65.63; H, 6.33; N, 7.33.

TOF mass $m/z$ 407.39 $(M + Na)^+$ $M_{cal}$ 384.17

*(c). Boc-Phe-Maba-OMe* ***5***. 3.714 g (14 mmol) of Boc-Phe-OH was dissolved in 30 mL of dry DCM in an ice−water bath. H-maba-OMe was isolated from 5.628 g (30 mmol) of the corresponding methyl ester hydrochloride by neutralization, and subsequent extraction with ethyl acetate and ethyl acetate extract was concentrated to 15 mL. It was then added to the reaction mixture, followed immediately by 2.888 g (14 mmol) of DCC and 1.891 g (14 mmol) of HOBt. The reaction mixture was allowed to come to room temperature and was stirred for 48 h. DCM was evaporated and the residue was dissolved in ethyl acetate (60 mL) and dicyclohexylurea (DCU) was filtered off. The organic layer was washed with 2 M HCl (3 × 50 mL), brine (2 × 50 mL), 1 M sodium carbonate (3 × 50 mL), and brine (2 × 50 mL) and dried over anhydrous sodium sulfate, and evaporated in a vacuum to yield compound **5** as a white solid. The product was purified by silica gel (100−200 mesh) using *n*-hexane−ethyl acetate (3:1) as the eluent.

Yield: 4.574 g (11.48 mmol, 86.56%).

$^1$H NMR ($CDCl_3$, 500 MHz, $\delta$ppm): 8.05 (s, 1H, Maba ring proton), 7.93 (s, 1H, Maba NH), 7.76−7.74 (d, 1H, $J$ = 10, Maba ring proton), 7.66−7.64 (d, 1H, $J$ = 10, Maba ring proton), 7.34 (m, 1H, Maba ring proton), 7.312−7.170 (m, 5H, phenyl ring protons), 5.15 (d, 1H, $J$ = 10, Phe NH), 4.46 (m, 1H, Phe C$\alpha$H), 3.89 (s, 3H, -OMe Hs), 3.16−3.14 (d, 2H, $J$ = 10 Hz, Phe C$\beta$H), 1.42 (s, 9H, Boc Hs). $^{13}$C NMR ($CDCl_3$, 125 MHz, $\delta$ppm): 168.76, 165.58, 136.46, 135.45, 129.87, 128.27, 128.05, 127.86, 126.15, 124.57, 123.42, 119.89, 51.20, 37.18, 27.24, FTIR (cm$^{-1}$): 3333.12, 3063.82, 2980.51, 1718.59, 1686.15, 1593.36, 1522.11, 1432.64, 1367.88, 1301.66, 1271.09, 1234.46, 1164.25, 1102.38, 1083.92, 1048.41, 1022.13. Anal. Calcd for $C_{22}H_{26}N_2O_5$ (398.45): C, 66.32; H, 6.58; N, 7.03. Found: C, 66.31; H, 6.56; N, 7.05.

*(d). Boc-Phe-Maba-OH* ***2***. To 4.382 g (11.0 mmol) of Boc-Phe-Maba-OMe, 25 mL of MeOH and 15 mL of 2 M NaOH were added, and the progress of saponification was monitored by thin layer chromatography (TLC). The reaction mixture was stirred. After 10 h, methanol was removed under a vacuum; the residue was dissolved in 50 mL of water and washed with diethyl ether (2 × 50 mL). Then the pH of the aqueous layer was adjusted to 2 using 1 M HCl, and it was extracted with ethyl acetate (3 × 50 mL). The extracts were pooled, dried over anhydrous sodium sulfate, and evaporated under a vacuum to obtain the compound as a white solid.

Yield 4.005 g (10.15 mmol, 92.3%).

Melting point: 170 °C.

$^1$H NMR (DMSO-$d_6$, 500 MHz, $\delta$ppm): 12.99 (b, 1H, COOH), 10.18 (s, 1H, Maba NH), 8.15 (s, 1H, Maba ring proton), 7.77−7.75 (d, 1H, $J$ = 10, Maba ring proton), 7.57−7.55 (d, 1H, $J$ = 10, Maba ring proton), 7.38 (m, 1H, Maba ring proton), 7.26−7.13 (m, 5H, phenyl ring protons), 7.12−7.11 (d, 1H, $J$ = 5, Phe NH), 4.26−4.21 (m, 1H, Phe C$\alpha$H), 2.95−2.91 (d, 1H, $J$ = 20 Hz, Phe C$\beta$H), 2.79−2.75 (d, 1H, $J$ = 20 Hz, Phe C$\beta$H), 1.25 (s, 9H, Boc Hs). $^{13}$C NMR (DMSO-$d_6$, 125 MHz, $\delta$ppm): 171.044, 167.11, 155.39, 139.10, 137.87, 131.25, 129.20, 128.99, 128.03, 126.28, 124.07, 123.33, 119.99, 78.10, 56.63, 37.31, 28.13. FTIR (cm$^{-1}$): 3297.96, 2982.59, 2928.18, 1683.92, 1547.43, 1397.10, 1259.57, 1217.22, 1166.72, 1050.72. Anal. Calcd for $C_{21}H_{24}N_2O_5$ (384.43): C, 65.61; H, 6.29; N, 7.29. Found: C, 65.63; H, 6.31; N, 7.28.

TOF mass $m/z$ 384.47 $(M)^+$ $M_{cal}$ 384.17


dx.doi.org/10.1021/cg201268x | *Cryst. Growth Des.* 2012, 12, 422−428

*(e). Boc-Phe-Paba-OMe* **6**. 3.714 g (14 mmol) of Boc-Phe-OH was dissolved in 30 mL of dry DCM in an ice−water bath. H-Paba-OMe was isolated from 5.628 g (30 mmol) of the corresponding methyl ester hydrochloride by neutralization, and subsequent extraction with ethyl acetate and ethyl acetate extract was concentrated to 15 mL. It was then added to the reaction mixture, followed immediately by 2.888 g (14 mmol) of DCC and 1.891 g (14 mmol) of HOBt. The reaction mixture was allowed to come to room temperature and was stirred for 48 h. DCM was evaporated and the residue was dissolved in ethyl acetate (60 mL) and DCU was filtered off. The organic layer was washed with 2 M HCl (3 × 50 mL), brine (2 × 50 mL), 1 M sodium carbonate (3 × 50 mL), and brine (2 × 50 mL) and dried over anhydrous sodium sulfate and evaporated in a vacuum to yield compound **6** as a white solid. The product was purified by silica gel (100−200 mesh) using *n*-hexane−ethyl acetate (3:1) as eluent.

Yield: 4.203 g (10.55 mmol, 75.36%).

$^1$H NMR ($CDCl_3$, 400 MHz, $\delta_{ppm}$): 8.10 (b, 1H, NH Paba), 7.97−7.95(d, 2H, $J$ = 8 Hz, paba ring protons), 7.47−7.45(d, 2H, $J$ = 8 Hz, paba ring protons), 7.29−7.26(m, 5H, phenyl ring protons), 5.10 (d, 1H, $J$ = 6 Hz, Phe NH), 4.46−4.46 (m, 1H, C$\alpha$H Phe), 3.89 (s, 3H, OMe), 3.16−3.14 (d, 2H, $J$ = 8 Hz, C$\beta$H Phe), 1.42 (s, 9H, Boc). $^{13}$C NMR ($CDCl_3$, 100 MHz, $\delta_{ppm}$): 170.238, 166.520, 155.927, 141.606, 136.371, 130.622, 129.201, 128.744, 127.075, 125.626, 118.942, 80.813, 56.634, 51.971, 38.270, 38.270, 28.211. FTIR ($cm^{-1}$): 3347, 2952, 1716, 1670, 1521, 1434, 1407, 1367, 1318, 1284, 1177, 1162, 1112.

Anal. calcd for $C_{22}H_{26}N_2O_5$ (398.45): C, 66.32; H, 6.58; N, 7.03.

Found: C, 66.37; H, 6.51; N, 7.06.

*(f). Boc-Phe-Paba-OH* **3**. To 4.183 g (10.5 mmol) of compound Boc-Phe-OMe, 25 mL of MeOH and 15 mL of 2 M NaOH were added, and the progress of saponification was monitored by thin layer chromatography (TLC). The reaction mixture was stirred. After 10 h, methanol was removed under vacuum; the residue was dissolved in 50 mL of water, and washed with diethyl ether (2 × 50 mL). Then the pH of the aqueous layer was adjusted to 2 using 1 M HCl and it was extracted with ethyl acetate (3 × 50 mL). The extracts were pooled, dried over anhydrous sodium sulfate, and evaporated under a vacuum to obtain compound **3** as a white solid.

Yield 3.740 g (9.73 mmol, 92.68%).

Melting point: 192 °C

$^1$H NMR (DMSO-$d_6$, 500 MHz, $\delta_{ppm}$): 12.78 (b, 1H, COOH), 10.33 (s,1H, NH Paba), 7.91−7.89 (d, 2H, $J$ = 10 Hz, paba ring protons), 7.71−7.69 (d, 2H, $J$ = 10 Hz, paba ring protons), 7.33−7.15 (m, 5H, phenyl ring protons), 6.55−6.53 (d,1H, $J$ = 10 Hz, NH Phe), 4.01 (m, 1H, C$_\alpha$H Phe), 3.01−2.98 (d, 1H, $J$ = 15 Hz C$\beta$H Phe), 2.85−2.82 (d, 1H, $J$ = 15 Hz C$\beta$H Phe), 1.32 (s, 9H, Boc). $^{13}$C NMR (DMSO-$d_6$, 125 MHz, $\delta_{ppm}$): 171.37, 166.89, 155.42, 142.92, 137.78, 131.18, 129.05, 128.09, 126.31, 118.55, 112.55,78.15, 56.66, 37.27, 28.13. FTIR ($cm^{-1}$): 3310, 2974, 2928, 1686, 1601, 1560, 1534, 1411, 1250, 1172.

Anal. Calcd for $C_{21}H_{24}N_2O_5$ (384.43): C, 65.61; H, 6.29; N, 7.29. Found: C, 65.68; H, 6.30; N, 7.26.

Tof mass $m/z$ 384.45 $(M)^+$ $M_{cal}$ 384.17

**NMR Spectroscopy.** All NMR studies were carried out on a Brüker AVANCE 500 MHz, and JNM-ECS 400 MHz spectrometer at 298 K. Compounds concentrations were in the range 1−10 mmol in $CDCl_3$ and $(CD_3)_2SO$.

**FTIR Spectroscopy.** All reported solid-state FTIR spectra were obtained with a Perkin-Elmer Spectrum RX1 spectrophotometer with the KBr disk technique.

**Mass Spectrometry.** Mass spectra were recorded on a Q-Tof Micro YA263 high-resolution (Waters Corporation) mass spectrometer by positive-mode electrospray ionization.

**Polarimeter.** Rudolph Research analytical instrument. Model Autopol IV polarimeter was used.

**$N_2$ Gas Adsorption Experiment.** Nitrogen adsorption/desorption isotherms were obtained using a Quantachrome Autosorb Automated Gas Sorption System at STP. Before the analysis, the samples were degassed at 40 °C for 4 h. The $N_2$ gas adsorption/desorption isotherms (STP) of the peptides were close to the type-III adsorption isotherm. From the $N_2$ gas adsorption at low $P/P_0$, the following pore size distribution of the sample was obtained using the NLDFT method. The pore size distribution curve of peptide **1** exhibits one peak at 3.02 nm. From the Brunauer−Emmett−Teller (BET) equation, the BET surface areas were calculated as 22 $m^2$ $g^{-1}$. This analysis was done for compound **2** also. The pore size distribution curve of peptide exhibits one peak at 2.84 nm. From the Brunauer−Emmett−Teller (BET) equation, the BET surface areas were calculated as 11 $m^2$ $g^{-1}$.

**Scanning Electron Microscopy.** The morphologies of the reported materials were investigated by field emission scanning electron microscopy (FE-SEM). For the SEM study, the corresponding peptide solution in methanol−water (1:1 v/v) at a concentration of 0.5 mM were drop-cast on microscopic glass slides, dried under a vacuum for 2 days, and coated with platinum. The micrographs were taken in an SEM apparatus (JEOL microscope JSM-6700F).

**X-ray Crystallography.** Intensity data were collected with MoK$\alpha$ radiation at 100 K using Bruker APEX-2 CCD diffractometer. Data were processed using the Bruker SAINT package and the structure solution and refinement procedures were performed using SHELX97.[18] The non-hydrogen atoms were refined with anisotropic thermal parameters. The hydrogen atoms were included in geometric positions and given thermal parameters equivalent to 1.5 times those of the atom to which they were attached. The data have been deposited at the Cambridge Crystallographic Data Centre with reference numbers CCDC 813384, 813385, and 813386 for peptides **1**, **2**, and **3** respectively.

## ■ ASSOCIATED CONTENT

### Ⓢ Supporting Information

Additional information as noted in the text; crystallographic information files. This information is available free of charge via the Internet at http://pubs.acs.org/.

## ■ AUTHOR INFORMATION


### Corresponding Author

*E-mail: deba_h76@yahoo.com, deba_h76@iiserkol.ac.in.


## ■ ACKNOWLEDGMENTS

This research was funded by the DST (SR/FT/CS-041/2009), New Delhi, India. S.M., P.J., and S.K.M. thank the C.S.I.R, New Delhi, India, for a fellowship.

## ■ REFERENCES


(1) Hecht, S.; Huc, I. *Foldamers: Structure, Properties, and Applications*; Wiley-VCH: Weinheim, 2007.

(2) (a) Haldar, D.; Schmuck, C. *Chem. Soc. Rev.* **2009**, *2*, 363−371. (b) Albrecht, M. *Chem. Rev.* **2001**, *101*, 3457−3498. (c) Katagiri, H.; Miyagawa, T.; Furusho, Y.; Yashima, E. *Angew. Chem., Int. Ed.* **2006**, *45*, 1741−1744. (d) Li, J.; Wisner, J. A.; Jennings, M. C. *Org. Lett.* **2007**, *9*, 3267−3269. (e) Ito, H.; Furusho, Y.; Hasegawa, T.; Yashima, E. *J. Am. Chem. Soc.* **2008**, *130*, 14008−14015. (f) Gan, Q.; Bao, C.; Kauffmann, B.; Grélard, A.; Xiang, J.; Liu, S.; Huc, I.; Jiang, H. *Angew. Chem., Int. Ed.* **2008**, *47*, 1715−1718. (g) Gan, Q.; Li, F.; Li, G.; Kauffmann, B.; Xiang, J.; Huc, I.; Jiang, H. *Chem. Commun.* **2010**, 297−299. (h) Haldar, D.; Jiang, H.; Léger, J.-M.; Huc, I. *Angew. Chem., Int. Ed.* **2006**, *45*, 5483−5486. (i) Baptiste, B.; Zhu, J.; Haldar, D.; Kauffmann, B.; Léger, J.-M.; Huc, I. *Chem. Asian J.* **2010**, *5*, 1364−1375. (j) Haldar, D.; Jiang, H.; Léger, J.-M.; Huc, I. *Tetrahedron* **2007**, *63*, 6322−6330.

(3) Gorbitz, C. H. *Chem.—Eur. J.* **2007**, *13*, 1022−1031.

(4) Schmuck, C.; Wennemers, H. *Highlights in Bioorganic Chemistry*; Wiley-VCH: Weinheim, 2004.

(5) (a) Cheng, R. P.; Gellman, S. H.; DeGrado, W. F. *Chem. Rev.* **2001**, *101*, 3219−3232. (b) Aravinda, S.; Shamala, N.; Roy, R. S.; Balaram, P. *Proc. Indian Acad. Sci.* **2003**, *115*, 373−400. (c) Das, A. K.; Haldar, D.; Hegde, R. P.; Shamala, N.; Banerjee, A. *Chem. Commun.*

**2005**, 1836−1838. (d) Haldar, D.; Banerjee, A.; Drew, M. G. B.; Das, A. K.; Banerjee, A. *Chem. Commun.* **2003**, 1406−1407.
(6) (a) Görbitz, C. H. *New J. Chem.* **2003**, *27*, 1789−1793. (b) Görbitz, C. H. *Curr. Opin. Solid State Mater. Sci.* **2002**, *6*, 109−116.
(7) (a) Brüggemann, J.; Bitter, S.; Müller, S.; Müller, W. M.; Müller, U. N.; Maier, M.; Lindner, W.; Vögtle, F. *Angew. Chem., Int. Ed.* **2007**, *46*, 254−259. (b) Feigel, M.; Ladberg, R.; Engels, S.; Herbst-Hirmer, R.; Fröhlich, R. *Angew. Chem., Int. Ed.* **2006**, *45*, 5698−5702. (c) Hunter, C. A.; Spitaleri, A.; Tomas, S. *Chem. Commun.* **2005**, 3691−3693. (d) Gabriel, G. J.; Sorey, S.; Iverson, B. L. *J. Am. Chem. Soc.* **2005**, *127*, 2637−2640. (e) Cherny, I.; Gazit, E. *Angew. Chem., Int. Ed.* **2008**, *47*, 4062−4069. (f) Cherny, I.; Gazit, E. *Angew. Chem.* **2008**, *120*, 4128−4136. (g) Tamamis, P.; Adler-Abramovich, L; Reches, M.; Marshall, K.; Sikorski, P.; Serpell, L.; Gazit, E; Archontis, G. *Biophys. J.* **2009**, *96*, 5020−5029. (h) Ulijn, R. V.; Smith, A. M. *Chem. Soc. Rev.* **2008**, *37*, 664−675.
(8) Delsuc, N.; Godde, F.; Kauffmann, B.; Léger, J.-M.; Huc, I. *J. Am. Chem. Soc.* **2007**, *129*, 11348−11349.
(9) Lin, J.; Wen, L.; Zang, S.; Su, Y.; Lu, Z.; Zhu, H.; Meng, Q. *Inorg. Chem. Commun.* **2007**, *10*, 74−76.
(10) (a) Angelici, G.; Castellucci, N.; Falini, G.; Huster, D.; Monari, M.; Tomasini, C. *Cryst. Growth Des.* **2010**, *10*, 923−929. (b) Angelici, G.; Falini, G.; Hofmann, H.-J.; Huster, D.; Monari, M.; Tomasini, C. *Angew. Chem., Int. Ed.* **2008**, *47*, 8075−8078. (c) Angelici, G.; Falini, G.; Hofmann, H.-J.; Huster, D.; Monari, M.; Tomasini, C. *Chem.—Eur. J.* **2009**, *15*, 8037−8048.
(11) (a) Jana, P.; Maity, S.; Maity, S. K.; Haldar, D. *Chem. Commun.* **2011**, *47*, 2092−2094. (b) Maity, S.; Kumar, P.; Haldar, D. *Soft Matter* **2011**, *7*, 5239−5245. (c) Maity, S.; Kumar, P.; Haldar, D. *Org. Biomol. Chem.* **2011**, *9*, 3787−3791. (d) Maity, S.; Jana, P.; Maity, S. K.; Haldar, D. *Langmuir* **2011**, *27*, 3835−3841.
(12) (a) Toniolo, C.; Palumbo, M. *Biopolymers* **1977**, *16*, 219−224. (b) Moretto, V.; Crisma, M.; Bonora, G. M.; Toniolo, C.; Balaram, H.; Balaram, P. *Macromolecules* **1989**, *22*, 2939−2944. (c) Haldar, D.; Banerjee, A. *Int. J. Pept. Res. Ther.* **2007**, *13*, 439−446.
(13) (a) Dado, G. P.; Gellman, S. H. *J. Am. Chem. Soc.* **1994**, *116*, 1054−1062. (b) Haldar, D.; Banerjee, A. *Int. J. Pept. Res. Ther.* **2006**, *12*, 341−348.
(14) Maji, S. K.; Velmurugan, D.; Razak, A.; Fun, H. K.; Banerjee, A. *Lett. Pept. Sci.* **2001**, *7*, 353−358.
(15) Baptiste, B.; Douat-Casassus, C.; Reddy, K. L.; Godde, F.; Huc, I. *J. Org. Chem.* **2010**, *75*, 7175−7185.
(16) Maity, S.; Jana, P.; Haldar, D. *CrystEngComm* **2011**, *13*, 3064−3071.
(17) (a) Jana, P.; Maity, S.; Haldar, D. *CrystEngComm* **2011**, *13*, 973−978. (b) Chandra, D.; Bhaumik, A. *J. Mater. Chem.* **2009**, *19*, 1901−1907.
(18) Sheldrick, G. M. *SHELX 97*; University of Göttingen: Germany, 1997.